Light quark pseudoscalar densities and anomaly matrix elements for η and η' mesons

Janardan P. Singh*

Physics Department, Faculty of Science, The M. S. University of Baroda, Vadodara 390 002, India

(Received 13 July 2013; published 12 November 2013)

Matrix elements of flavor-diagonal light quark pseudoscalar densities and axial anomaly operators between vacuum and η and η' meson states have been determined. This has been done by evaluating current-current correlators of octet-octet and octet-singlet axial currents using QCD sum rules. The numerical values obtained for the matrix elements compare well with those obtained in the current literature.

DOI: 10.1103/PhysRevD.88.096005 PACS numbers: 11.15.Tk, 11.40.Ex, 12.38.Lg, 14.40.Be

I. INTRODUCTION

Matrix elements of pseudoscalar density operators between vacuum and η and η' mesons are useful in the study of processes involving the production and decay of these mesons. In particular, they play an important role in semileptonic and nonleptonic B-meson decays involving η and η' mesons [1–8]. These, as well as the anomaly matrix elements, are useful in the discussion of pseudoscalar glueballs [9]. The latter have also been used in the study of the gluonic components of η-η' mesons [10]. These matrix elements also appear in the discussion of two-parton light-cone distribution functions of these mesons where there is no direct relation between the coupling constants of twist-3 operators and those of twist-2 operators for η and η' mesons [11]. In this work, we will determine the matrix elements

$$\langle 0|m_q\bar{q}i\gamma_5 q|\eta,\eta'\rangle, \quad q=u,d,s \tag{1}$$

and

$$\left\langle 0\left|\frac{\alpha_s}{4\pi}G^a_{\mu\nu}\tilde{G}^{a\mu\nu}\right|\eta,\eta'\right\rangle \tag{2}$$

using the QCD sum rule. For this, we first consider the correlators of two axial vector currents,

$$\Pi^{ab}_{\mu\nu}=i\int d^4x e^{iqx}\langle 0|T\{J^a_{\mu 5}(x),J^b_{\nu 5}(0)\}|0\rangle; \quad (a,b=8,0), \tag{3}$$

where

$$\begin{aligned} J^8_{\mu 5}&=\frac{1}{\sqrt{6}}(\bar{u}\gamma_\mu\gamma_5 u+\bar{d}\gamma_\mu\gamma_5 d-2\bar{s}\gamma_\mu\gamma_5 s),\\ J^0_{\mu 5}&=\frac{1}{\sqrt{3}}(\bar{u}\gamma_\mu\gamma_5 u+\bar{d}\gamma_\mu\gamma_5 d+\bar{s}\gamma_\mu\gamma_5 s). \end{aligned} \tag{4}$$

We had earlier considered the correlators of Eq. (3) in Ref. [12] and determined the decay constants of η and η' mesons for the above octet and singlet currents defined by

$$\langle 0|J^a_{\mu 5}|P(p)\rangle=if^a_P p_\mu; \qquad P=\eta,\eta' \tag{5}$$

in the limit $m_u=m_d=0$. In this work, we determine their values while keeping all the quark masses nonzero. In the current literature, the decay constants f^a_P are parameterized as

$$\begin{pmatrix} f^8_\eta & f^0_\eta \\ f^8_{\eta'} & f^0_{\eta'}\end{pmatrix}=\begin{pmatrix} f_8\cos\theta_8 & -f_0\sin\theta_0 \\ f_8\sin\theta_8 & f_0\cos\theta_0\end{pmatrix}. \tag{6}$$

On forming the divergences of the polarization tensor $\Pi^{ab}_{\mu\nu}(q)$ with the momentum, we get

$$q^\mu\Pi^{ab}_{\mu\nu}(q)q^\nu=-P^{ab}_L(q^2)q^2, \tag{7}$$

where $P^{ab}_L(q^2)$ is free from kinematic singularities. The divergences of currents are given as

$$\begin{aligned} \partial^\mu J^8_{\mu 5}&=\frac{2i}{\sqrt{6}}(m_u\bar{u}\gamma_5 u+m_d\bar{d}\gamma_5 d-2m_s\bar{s}\gamma_5 s),\\ \partial^\mu J^0_{\mu 5}&=\frac{2i}{\sqrt{3}}(m_u\bar{u}\gamma_5 u+m_d\bar{d}\gamma_5 d+m_s\bar{s}\gamma_5 s),\\ &\quad-\frac{\sqrt{3}\alpha_s}{4\pi}G^a_{\mu\nu}\tilde{G}^{a\mu\nu}, \end{aligned} \tag{8}$$

where we have defined the dual field strength tensor as

$$\tilde{G}^{a\mu\nu}=\frac{1}{2}\varepsilon^{\mu\nu\rho\sigma}G^a_{\rho\sigma}, \qquad \varepsilon^{0123}=+1. \tag{9}$$

We will assume isospin symmetry in the quark matrix elements,

$$\langle 0|m_u\bar{u}i\gamma_5 u|\eta\rangle=\langle 0|m_d\bar{d}i\gamma_5 d|\eta\rangle\equiv m_q A_q, \tag{10}$$

$$\langle 0|m_u\bar{u}i\gamma_5 u|\eta'\rangle=\langle 0|m_d\bar{d}i\gamma_5 d|\eta'\rangle\equiv m_q A'_q, \tag{11}$$

and call

$$\langle 0|m_s\bar{s}i\gamma_5 s|\eta\rangle\equiv m_s A_s, \tag{12}$$

$$\langle 0|m_s\bar{s}i\gamma_5 s|\eta'\rangle\equiv m_s A'_s, \tag{13}$$

while the anomaly matrix elements will be denoted as

*janardanmsu@yahoo.com

$$\left\langle 0 \left| \frac{\alpha_s}{4\pi} G^a_{\mu\nu} \tilde{G}^{a\mu\nu} \right| \eta \right\rangle \equiv A_G, \tag{14}$$

$$\left\langle 0 \left| \frac{\alpha_s}{4\pi} G^a_{\mu\nu} \tilde{G}^{a\mu\nu} \right| \eta' \right\rangle \equiv A'_G. \tag{15}$$

In Eqs. (10) and (11), m_q is the average of the up- and down-quark masses. The strange-quark matrix elements A_s and A'_s will be determined in the limit $m_q = 0$. For this, we require the values of meson masses m_η and $m_{\eta'}$ also in the same limit. From the diagonalization of the m_η-$m_{\eta'}$ mass matrix [13], one obtains values for η and η' masses:

$$m^2_{\eta',\eta} = (m_K^2 + \tilde{m}^2_{\eta_0}/2) \pm \frac{1}{2}\sqrt{\left(2m_K^2 - 2m_\pi^2 - \frac{1}{3}\tilde{m}^2_{\eta_0}\right)^2 + \frac{8}{9}\tilde{m}^4_{\eta_0}}. \tag{16}$$

Here, $\tilde{m}^2_{\eta_0}$ is the gluonic mass term having a rigorous interpretation through the Witten-Veneziano mass formula [14,15]. On taking the value $\tilde{m}^2_{\eta_0} = 0.73$ GeV^2, Eq. (16) agrees with the physical masses within a 10% range. The dependence of m_K and m_π on light quark masses is well known [16]. From this, we find that m_η decreases by 2.2% while $m_{\eta'}$ decreases by 0.65% on setting $m_q = 0$. Using this result for the experimental masses $m_\eta = 0.547$ GeV and $m_{\eta'} = 0.958$ GeV, we find that the values of η and η' masses are

$$\tilde{m}_\eta = 0.535 \text{ GeV}, \qquad \tilde{m}_{\eta'} = 0.952 \text{ GeV} \tag{17}$$

in a world where $m_q = 0$. We will assume η and η' to be made up of only light quarks with no mixing with the $c\bar{c}$ system or any glueball state. Among half a dozen functions considered in Ref. [12], we will consider here sum rules only for P_L^{88} and P_L^{08}. Sum rules for these functions were independent of any instanton contribution, and the quality of the fit of the phenomenological side with the OPE side was best obtained for these functions. In addition to this, these sum rules give us sufficient information for our purpose.

To use the method of the QCD sum rule for this purpose, as is well known, one calculates P_L^{ab} using OPE on the one hand, and it is evaluated phenomenologically using a dispersion integral on the other hand. The Borel transform of the two sides is matched over an appropriately chosen Borel window. After the Borel transform, the phenomenological side is dominated by the ground-state contribution, while the resonance and the continuum contributions are parameterized by the loop diagrams of the OPE side with a continuum threshold. Matching of the two sides determines the phenomenological quantity of interest in terms of QCD parameters, which include vacuum condensates.

II. SUM RULES

From P_L^{88}, we get the following sum rule, which is an extension of the corresponding Eq. (33) in Ref. [12], with $m_q \neq 0$, as

$$\begin{aligned} &K_{88} + \frac{8}{3}\frac{1}{m_\eta^2}(m_q A_q - m_s A_s)^2 e^{-m_\eta^2/M^2} + \frac{8}{3}\frac{1}{m_{\eta'}^2}(m_q A'_q - m_s A'_s)^2 e^{-m_{\eta'}^2/M^2} \\ &= \frac{1}{\pi^2} m_s^2 M^2 \left\{1 + \frac{\alpha_s}{\pi}\left(\frac{17}{3} + 2\gamma - 2ln\frac{M^2}{\mu^2}\right)\right\} E_0\left(\frac{W^2}{M^2}\right) - \frac{8}{3} m_s \langle \bar{s}s \rangle + \frac{16}{3} m_s^3 \frac{\langle \bar{s}s \rangle}{M^2} - \frac{2}{3}\frac{m_s^2}{M^2}\left\langle \frac{\alpha_s}{\pi} G^2 \right\rangle \\ &\quad - \frac{64}{9}\pi^2 \frac{\alpha_s}{\pi}\frac{m_s^2}{M^4}\kappa_s \langle \bar{s}s \rangle^2 - \frac{4}{3}\frac{m_s^3}{M^4}\langle \bar{s} g_s \sigma . Gs \rangle - \frac{4}{3} m_q \langle \bar{q}q \rangle + \frac{1}{2\pi^2} m_q^2 M^2 \left\{1 + \frac{\alpha_s}{\pi}\left(\frac{17}{3} + 2\gamma - 2ln\frac{M^2}{\mu^2}\right)\right\} E_0\left(\frac{W^2}{M^2}\right) \\ &\quad - \frac{1}{3}\frac{m_q^2}{M^2}\left\langle \frac{\alpha_s}{\pi} G^2 \right\rangle - \frac{32}{9}\pi^2 \frac{\alpha_s}{\pi}\frac{m_q^2}{M^4}\kappa \langle \bar{q}q \rangle^2. \end{aligned} \tag{18}$$

In the above equation, M is the Borel mass parameter; μ is the renormalization point; κ and κ_s are different from 1 to account for contributions from beyond the ground-state factorization of four-quark condensate [17], not considered in Ref. [12]; γ is Euler's constant; W is the continuum threshold; $E_0(x) = 1 - e^{-x}$; and $\langle \bar{u}u \rangle = \langle \bar{d}d \rangle = \langle \bar{q}q \rangle$. As explained in Ref. [12], K_{88} is the residue of a spurious pole in P_L^{88} at $q^2 = 0$, which is introduced due to the approximate form of P_L^{88} obtained by OPE. For up- and down-quark contributions to the rhs of the sum rule, we have retained terms up to quadratic in m_q, since the linear term will contribute only to K_{88}. Also, clearly we have relations such as $\frac{8}{3}\frac{1}{m_\eta^2}(m_q A_q - m_s A_s)^2 = m_\eta^2 (f_\eta^8)^2$, etc. [12]. Upon setting $m_q = 0$, we get the sum rule

$$\begin{aligned} &\tilde{K}_{88} + \frac{8}{3}\frac{1}{\tilde{m}_\eta^2}(m_s A_s)^2 e^{-\tilde{m}_\eta^2/M^2} + \frac{8}{3}\frac{1}{\tilde{m}_{\eta'}^2}(m_s A'_s)^2 e^{-\tilde{m}_{\eta'}^2/M^2} \\ &= \frac{1}{\pi^2} m_s^2 M^2 \left\{1 + \frac{\alpha_s}{\pi}\left(\frac{17}{3} + 2\gamma - 2ln\frac{M^2}{\mu^2}\right)\right\} E_0\left(\frac{W^2}{M^2}\right) \\ &\quad - \frac{8}{3} m_s \langle \bar{s}s \rangle + \frac{16}{3} m_s^3 \frac{\langle \bar{s}s \rangle}{M^2} - \frac{2}{3}\frac{m_s^2}{M^2}\left\langle \frac{\alpha_s}{\pi} G^2 \right\rangle \\ &\quad - \frac{64}{9}\pi^2 \frac{\alpha_s}{\pi}\frac{m_s^2}{M^4}\kappa_s \langle \bar{s}s \rangle^2 - \frac{4}{3}\frac{m_s^3}{M^4}\langle \bar{s} g_s \sigma . Gs \rangle. \end{aligned} \tag{19}$$

We have used the following constants in Eqs. (18) and (19) [12,18]:

$$\alpha_s(1\ \mathrm{GeV}^2) = 0.5, \qquad a = -(2\pi)^2\langle\bar{q}q\rangle = 0.55\ \mathrm{GeV}^3,$$
$$\langle\bar{s}s\rangle = 0.8\langle\bar{q}q\rangle, \qquad b = \langle g_s^2 G^2\rangle = 0.5\ \mathrm{GeV}^4,$$
$$\langle\bar{s}g_s\sigma.Gs\rangle = m_0^2\langle\bar{s}s\rangle \quad \text{with} \quad m_0^2 = 0.8\ \mathrm{GeV}^2,$$
$$m_s = 0.153\ \mathrm{GeV}, \qquad m_q = 0.005\ \mathrm{GeV},$$
$$\kappa = \kappa_s = 2.5, \qquad \mu = 1\ \mathrm{GeV} \quad \text{and} \quad W^2 = 2.3\ \mathrm{GeV}^2. \tag{20}$$

Equation (19) was used in Ref. [12] with $\kappa_s = 1$ and physical masses of η and η'. The range of M^2 over which the two sides of a sum rule are matched is decided as follows: The smaller the M^2, the more important are the higher-dimensional operators, which puts a lower limit on M^2; while the larger the M^2, the more important are the resonance and continuum states, which puts an upper limit on M^2. We fit the two sides of each of Eqs. (18) and (19) over a range $1.0\ \mathrm{GeV}^2 < M^2 < 1.7\ \mathrm{GeV}^2$. It is observed that in the specified range, the operators of highest dimension included in the OPE are contributing less than 1%, and the resonance and the continuum states, transferred on the OPE side and contained in $E_0(W^2/M^2)$ in perturbative terms, are contributing less than 25% to the OPE side result. This is well within the accepted criteria for the standard treatment of QCD sum rules [18]. We have shown the plots of the rhs of Eq. (18) and a fit as the lhs in Fig. 1. Also shown are the rhs of Eq. (19) along with a fit as the lhs in Fig. 2. Equation (18) gives slightly changed results for the decay constants:

$$f_\eta^8 = 159.1\ \mathrm{MeV}\ (165.6\ \mathrm{MeV}),$$
$$f_{\eta'}^8 = -66.4\ \mathrm{MeV}\ (-62.2\ \mathrm{MeV}), \tag{21}$$

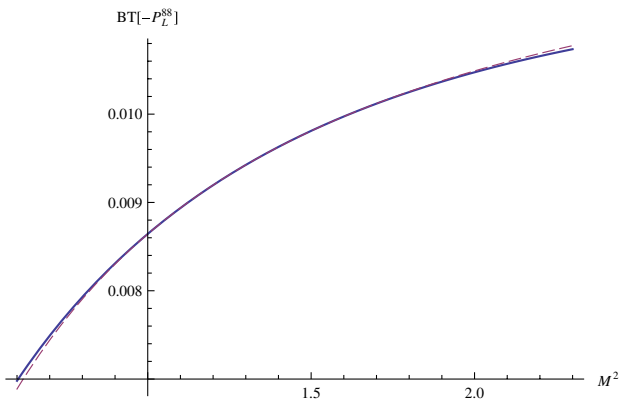

FIG. 1 (color online). Plots of the two sides of Eq. (18) (called $BT[-P_L^{88}]$) as a function of M^2 for $m_q = 5$ MeV. The best fit in the region $1.0\ \mathrm{GeV}^2 \le M^2 \le 1.7\ \mathrm{GeV}^2$ corresponds to $(f_\eta^8)^2 m_\eta^2 = 0.00758\ \mathrm{GeV}^4$ and $(f_{\eta'}^8)^2 m_{\eta'}^2 = 0.00404\ \mathrm{GeV}^4$. $\chi = 4.7 \times 10^{-5}$ ($N = 20$) for the fit in the designated interval.

where the quantity in the bracket is from Ref. [12]. This gives us $f_8 = 172.4$ MeV, $\theta_8 = -22.6°$. If we show the quality of the fit by χ^2, defined as

$$\chi^2 = \frac{1}{N}\sum_{i=1}^{N}\frac{[f(x_i) - f_{\mathrm{fit}}(x_i)]^2}{[f(x_i) + f_{\mathrm{fit}}(x_i)]^2}, \tag{22}$$

where $f(x_i)$ stands for the rhs of Eqs. (18) and (19) and $f_{\mathrm{fit}}(x_i)$ for the lhs of the corresponding equation, we find that for $N = 20$, $\chi = 4.7 \times 10^{-5}$ for both the curves. The result of the fit for Eq. (18) gives

$$\frac{8}{3}\frac{1}{m_\eta^2}(m_q A_q - m_s A_s)^2 = 7.58 \times 10^{-3}\ \mathrm{GeV}^4,$$
$$\frac{8}{3}\frac{1}{m_{\eta'}^2}(m_q A_q' - m_s A_s')^2 = 4.04 \times 10^{-3}\ \mathrm{GeV}^4, \tag{23}$$
$$K_{88} = 1.41 \times 10^{-3}\ \mathrm{GeV}^4,$$

while that for Eq. (19) gives

$$\frac{8}{3}\frac{1}{\tilde{m}_\eta^2}(m_s A_s)^2 = 7.52 \times 10^{-3}\ \mathrm{GeV}^4,$$
$$\frac{8}{3}\frac{1}{\tilde{m}_{\eta'}^2}(m_s A_s')^2 = 4.22 \times 10^{-3}\ \mathrm{GeV}^4, \tag{24}$$
$$\tilde{K}_{88} = 1.20 \times 10^{-3}\ \mathrm{GeV}^4.$$

Equation (19) was obtained from Eq. (18) by setting $m_q = 0$ consistently on both sides of the equation, and this includes the theoretical values of $\tilde{m}_\eta^2$ and $\tilde{m}_{\eta'}^2$ as well in the same limit. Hence, Eqs. (23) and (24), obtained from fittings of Eqs. (18) and (19), respectively, are two self-consistent independent algebraic equations. As is shown below for A_G and A_G' [see Eqs. (28) and (30) below] following a similar procedure, taking the limit $m_q = 0$

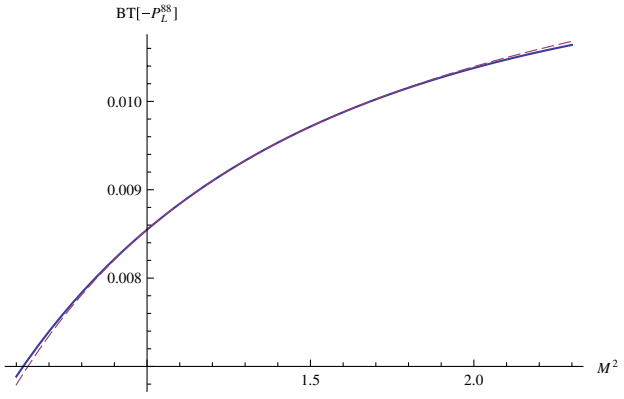

FIG. 2 (color online). Plots of the two sides of Eq. (19) (called $BT[-P_L^{88}]$) as a function of M^2 for $m_q = 0$. The best fit in the region $1.0\ \mathrm{GeV}^2 \le M^2 \le 1.7\ \mathrm{GeV}^2$ corresponds to $(f_\eta^8)^2\tilde{m}_\eta^2 = 0.00752\ \mathrm{GeV}^4$ and $(f_{\eta'}^8)^2\tilde{m}_{\eta'}^2 = 0.00422\ \mathrm{GeV}^4$. The masses $\tilde{m}_\eta$ and $\tilde{m}_{\eta'}$ are the phenomenological masses obtained for $m_q = 0$ [see Eq. (17)]. $\chi = 4.7 \times 10^{-5}$ for the fit in the designated interval.

does not change these matrix elements in a significant way. We solve Eqs. (23) and (24) to obtain the following results:

$$\begin{aligned} -m_s A_s &= 0.02841\ \text{GeV}^3, \\ m_s A'_s &= 0.03786\ \text{GeV}^3, \\ m_q A_q &= 7.45 \times 10^{-4}\ \text{GeV}^3, \\ m_q A'_q &= 5.53 \times 10^{-4}\ \text{GeV}^3. \end{aligned} \tag{25}$$

The sign of $m_s A_s$ is fixed from the requirement that in the limit of $m_q = 0$, $-m_s A_s = \frac{\sqrt{6}}{4} f_\eta^8 m_\eta^2$, which is positive. Equation (24) gives us $f_8 = 175.9$ MeV and $\theta_8 = -22.8°$. From P_L^{08}, we get the following sum rule, which is an extension of the corresponding Eq. (39) in Ref. [12] with $m_q \neq 0$:

$$\begin{aligned} &K_{08} + \frac{8\sqrt{2}}{3m_\eta^2}(m_q A_q - m_s A_s) \times \left(m_q A_q + \frac{1}{2} m_s A_s - \frac{3}{4} A_G\right) e^{-m_\eta^2/M^2} + \frac{8\sqrt{2}}{3m_{\eta'}^2}(m_q A'_q - m_s A'_s) \times \left(m_q A'_q + \frac{1}{2} m_s A'_s - \frac{3}{4} A'_G\right) e^{-m_{\eta'}^2/M^2} \\ &= \frac{3}{\sqrt{2}\pi^2}\left(\frac{\alpha_s}{\pi}\right)^2 m_s^2 M^2 \left(\frac{7}{4} - \frac{1}{2} ln\frac{M^2}{\mu^2}\right) E_0\left(\frac{W^2}{M^2}\right) - \frac{1}{\sqrt{2}\pi^2} m_s^2 M^2 \left\{1 + \frac{\alpha_s}{\pi}\left(\frac{17}{3} + 2\gamma - 2ln\frac{M^2}{\mu^2}\right)\right\} E_0\left(\frac{W^2}{M^2}\right) \\ &\quad + \frac{4\sqrt{2}}{3} m_s \langle \bar{s}s \rangle - 2\sqrt{2}\left(\frac{\alpha_s}{\pi}\right)^2 m_s \langle \bar{s}s \rangle \left(\gamma - ln\frac{M^2}{\mu^2}\right) + \frac{\sqrt{2}}{3}\frac{m_s^2}{M^2}\left\langle \frac{\alpha_s}{\pi} G^2 \right\rangle + \frac{1}{\sqrt{2}}\frac{\alpha_s}{\pi}\frac{m_s^2}{M^2}\left\langle \frac{\alpha_s}{\pi} G^2 \right\rangle \left(1 - \gamma + ln\frac{M^2}{\mu^2}\right) \\ &\quad - \frac{8\sqrt{2}}{3}\frac{m_s^3 \langle \bar{s}s \rangle}{M^2} - \sqrt{2}\frac{\alpha_s}{\pi}\frac{m_s}{M^2}\langle \bar{s} g_s \sigma . Gs \rangle + \frac{32\sqrt{2}}{9}\pi^2 \frac{\alpha_s}{\pi}\frac{m_s^2}{M^4}\kappa_s \langle \bar{s}s \rangle^2 + \frac{2\sqrt{2}}{3}\frac{m_s^3}{M^4}\langle \bar{s} g_s \sigma . Gs \rangle \\ &\quad - \frac{3}{\sqrt{2}\pi^2}\left(\frac{\alpha_s}{\pi}\right)^2 m_q^2 M^2 \left(\frac{7}{4} - \frac{1}{2} ln\frac{M^2}{\mu^2}\right) E_0\left(\frac{W^2}{M^2}\right) + \frac{1}{\sqrt{2}\pi^2} m_q^2 M^2 \left\{1 + \frac{\alpha_s}{\pi}\left(\frac{17}{3} + 2\gamma - 2ln\frac{M^2}{\mu^2}\right)\right\} E_0\left(\frac{W^2}{M^2}\right) \\ &\quad - \frac{4\sqrt{2}}{3} m_q \langle \bar{q}q \rangle + 2\sqrt{2}\left(\frac{\alpha_s}{\pi}\right)^2 m_q \langle \bar{q}q \rangle \left(\gamma - ln\frac{M^2}{\mu^2}\right) - \frac{\sqrt{2}}{3}\frac{m_q^2}{M^2}\left\langle \frac{\alpha_s}{\pi} G^2 \right\rangle - \frac{1}{\sqrt{2}}\frac{\alpha_s}{\pi}\frac{m_q^2}{M^2}\left\langle \frac{\alpha_s}{\pi} G^2 \right\rangle \left(1 - \gamma + ln\frac{M^2}{\mu^2}\right) \\ &\quad + \sqrt{2}\frac{\alpha_s}{\pi}\frac{m_q}{M^2}\langle \bar{q} g_s \sigma . Gq \rangle - \frac{32\sqrt{2}}{9}\pi^2 \frac{\alpha_s}{\pi}\frac{m_q^2}{M^4}\kappa \langle \bar{q}q \rangle^2. \end{aligned} \tag{26}$$

With the constants as given by Eq. (20), we have fitted Eq. (26) in the range $1.0\ \text{GeV}^2 < M^2 < 1.9\ \text{GeV}^2$ and displayed it in Fig. 3. The upper end of the range of M^2 for this fit is kept somewhat higher than that for the fit of P_L^{88}, because the required fit is better on the upper-end side and not so well on the lower-end side, as is clear from a comparison of Fig. 3 with Fig. 1. In the next section, we have analyzed the effect of variation of the range of M^2 over which fitting has been carried out. In this case also, the contribution of the highest-dimensional operator has been found to be less than 1%, while the resonance and continuum contribution is less than 25% to the OPE side result. The quality of fit is somewhat poor: $\chi = 1.3 \times 10^{-3}$. From the fit we get

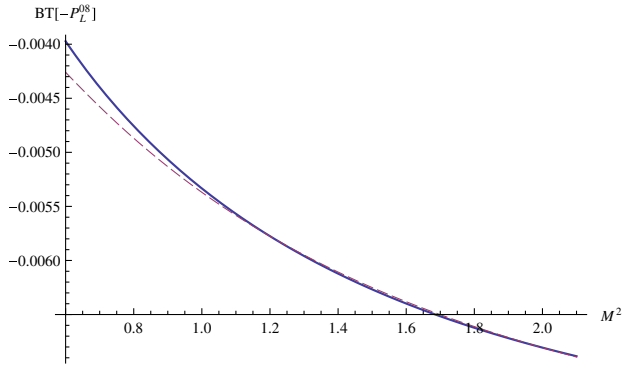

FIG. 3 (color online). Plots of the two sides of Eq. (26) (called $BT[-P_L^{08}]$) as a function of M^2 for $m_q = 5$ MeV. The best fit in the region $1.0\ \text{GeV}^2 \leq M^2 \leq 1.9\ \text{GeV}^2$ corresponds to $f_\eta^0 f_\eta^8 m_\eta^2 = 4.64 \times 10^{-4}\ \text{GeV}^4$ and $f_{\eta'}^0 f_{\eta'}^8 m_{\eta'}^2 = -6.414 \times 10^{-3}\ \text{GeV}^4$. $\chi = 1.29 \times 10^{-3}$ ($N = 20$) for the fit in the designated interval.

$$\begin{aligned} &\frac{8\sqrt{2}}{3m_\eta^2}(m_q A_q - m_s A_s)\left(m_q A_q + \frac{1}{2} m_s A_s - \frac{3}{4} A_G\right) \\ &\quad = 4.64 \times 10^{-4}\ \text{GeV}^4, \\ &\frac{8\sqrt{2}}{3m_{\eta'}^2}(m_q A'_q - m_s A'_s)\left(m_q A'_q + \frac{1}{2} m_s A'_s - \frac{3}{4} A'_G\right) \\ &\quad = -6.414 \times 10^{-3}\ \text{GeV}^4, \\ &K_{08} = -3.152 \times 10^{-3}\ \text{GeV}^4. \end{aligned} \tag{27}$$

P_L^{88} and P_L^{08} provide two independent sum rules in which the phenomenological side of P_L^{08} contains two additional parameters, A_G and A'_G, not present in P_L^{88}. In both the sum rules, the same parameters, including condensates and the continuum threshold have been used, although the range of the fit of M^2 is slightly larger for P_L^{08}. Once the four parameters, namely $m_q A_q$, $m_q A'_q$, $m_s A_s$ and $m_s A'_s$, have been determined from the P_L^{88} sum rule, this information

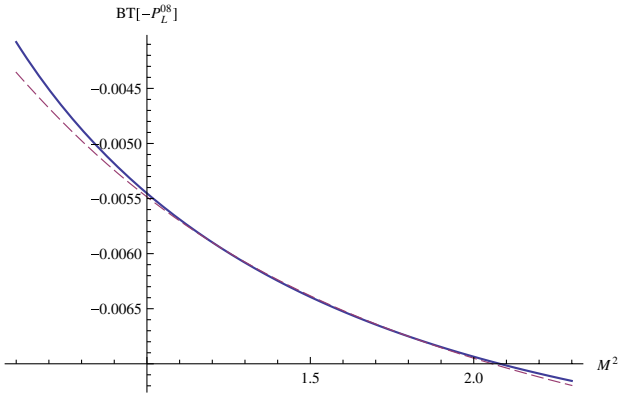

FIG. 4 (color online). Plots of the two sides of Eq. (26) (called $BT[-P_L^{08}]$) as a function of M^2 for $m_q = 0$. The best fit in the region 1.0 GeV$^2 \le M^2 \le$ 1.9 GeV^2 corresponds to $f_\eta^0 f_\eta^8 \tilde{m}_\eta^2 = 7.3 \times 10^{-4}$ GeV^4 and $f_{\eta'}^0 f_{\eta'}^8 \tilde{m}_{\eta'}^2 = -6.689 \times 10^{-3}$ GeV^4. The masses $\tilde{m}_\eta$ and $\tilde{m}_{\eta'}$ are the phenomenological masses obtained for $m_q = 0$ [see Eq. (17)]. $\chi = 9.97 \times 10^{-4}$ ($N = 20$) for the fit in the designated interval.

can be fed into the P_L^{08} sum rule to determine A_G and A_G'. From Eqs. (25) and (27), we get

$$A_G = -0.02197 \text{ GeV}^3, \qquad A_G' = -0.03704 \text{ GeV}^3. \tag{28}$$

Equation (26) with $m_q = 0$ on both sides of the equation has also been analyzed in a similar way, and the fit has been displayed in Fig. 4. For this fit, $\chi = 1.0 \times 10^{-3}$. This fit gives

$$\begin{aligned} \frac{8\sqrt{2}}{3\tilde{m}_\eta^2} m_s A_s \left(\frac{1}{2} m_s A_s - \frac{3}{4} A_G\right) &= -7.3 \times 10^{-3} \text{ GeV}^4, \\ \frac{8\sqrt{2}}{3\tilde{m}_{\eta'}^2} m_s A_s' \left(\frac{1}{2} m_s A_s' - \frac{3}{4} A_G'\right) &= 6.69 \times 10^{-3} \text{ GeV}^4, \\ \tilde{K}_{08} &= -3.33 \times 10^{-3} \text{ GeV}^4. \end{aligned} \tag{29}$$

Upon substituting $m_s A_s$ and $m_s A_s'$ from Eq. (25), we get

$$A_G = -0.02199 \text{ GeV}^3, \qquad A_G' = -0.03616 \text{ GeV}^3. \tag{30}$$

This shows that while A_G remains practically unchanged, $|A_G'|$ decreases by $\approx 2.4\%$ from the values given by Eq. (28). We will check the sensitivity of our result on m_s later. We also find that Eq. (27) gives

$$f_0 = 105.7 \text{ MeV}, \qquad \theta_0 = -5.3^\circ, \tag{31}$$

while Eq. (29) gives

$$f_0 = 110.0 \text{ MeV}, \qquad \theta_0 = -8.1^\circ, \tag{32}$$

compared to $f_0 = 142.3$ MeV and $\theta_0 = -11.1^\circ$ [12]. Part of the reason for this significant change is the use of $\tilde{m}_\eta$ and $\tilde{m}_{\eta'}$ as against m_η and m_η used in Ref. [12] and different κ and κ_s in this work, and part of the reason is a small mistake in the numerical evaluation of the mixed condensate term in our previous work [12].

III. ANALYSIS AND DISCUSSION

In order to show that our results are sufficiently sensitive to distinguish the cases with $m_q \neq 0$ from those with $m_q = 0$, we have displayed the two curves (with $m_q =$ 5 MeV and $m_q = 0$) on the same plot in Fig. 5 for $\text{BT}[-P_L^{88}]$ and in Fig. 6 for $\text{BT}[-P_L^{08}]$, where BT stands for Borel transform.

We have also checked the sensitivities of our results to variations of the parameters used in the computation. We have shown the plots of $\text{BT}[-P_L^{88}]$ in Fig. 7 as $\langle \bar{q}q \rangle$ is varied by 20% and $\langle \frac{\alpha_s}{\pi} G^2 \rangle$ is varied by 40%; in Fig. 8 as both α_s and m_s are varied by 10% each; and in Fig. 9 as the continuum threshold W^2 is varied by ± 0.1 GeV^2. Plots of $\text{BT}[-P_L^{08}]$ are shown in Figs. 10–12, respectively, for similar variations of parameters. The quark pseudoscalar densities and anomaly matrix elements for η and η' mesons for each one of these variations have been determined separately. We have also determined these matrix elements

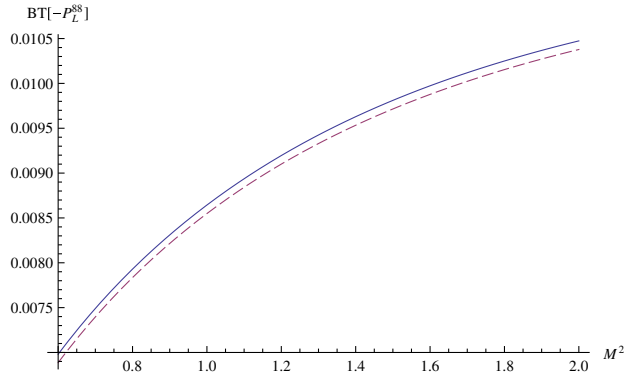

FIG. 5 (color online). Plots of the two forms of $BT[-P_L^{88}]$ as a function of M^2 for $m_q = 5$ MeV (solid line) and for $m_q = 0$ (dashed line).

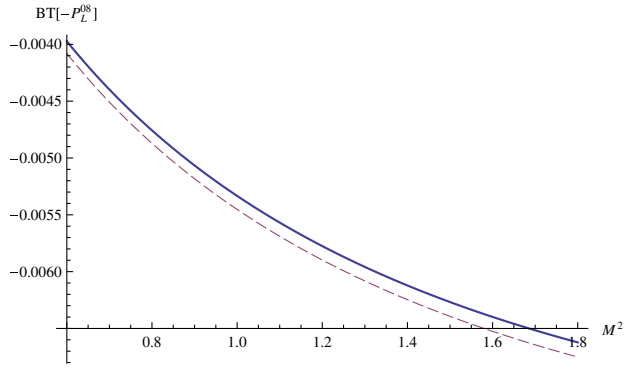

FIG. 6 (color online). Plots of the two forms of $BT[-P_L^{08}]$ as a function of M^2 for $m_q = 5$ MeV (solid line) and for $m_q = 0$ (dashed line).

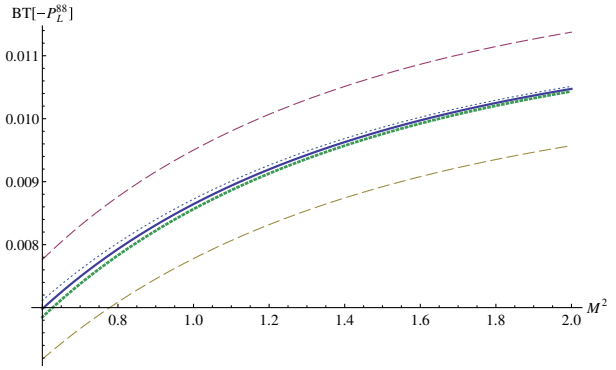

FIG. 7 (color online). Plots of $BT[-P_L^{88}]$ as a function of M^2 for normal (solid), quark condensate changed by 20% (dashed), and gluon condensate changed by 40% (dotted).

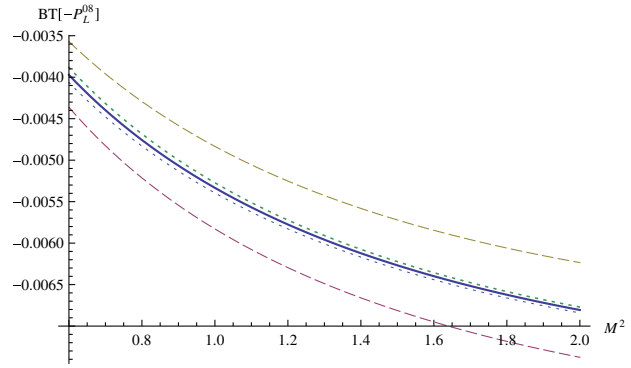

FIG. 10 (color online). Plots of $BT[-P_L^{08}]$ as a function of M^2 for normal (solid), quark condensate changed by 20% (dashed), and gluon condensate changed by 40% (dotted).

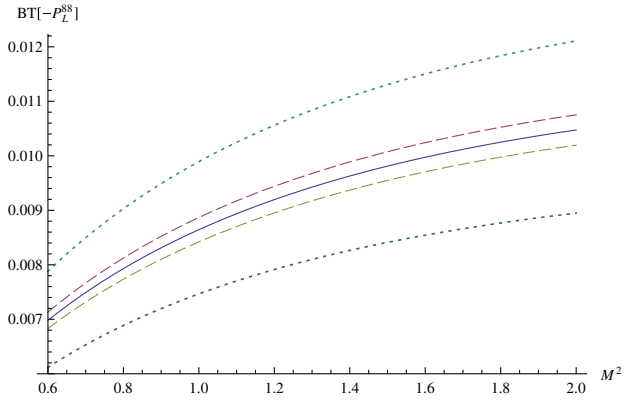

FIG. 8 (color online). Plots of $BT[-P_L^{88}]$ as a function of M^2 for normal (solid), α_s changed by 10% (dashed), and m_s changed by 10% (dotted).

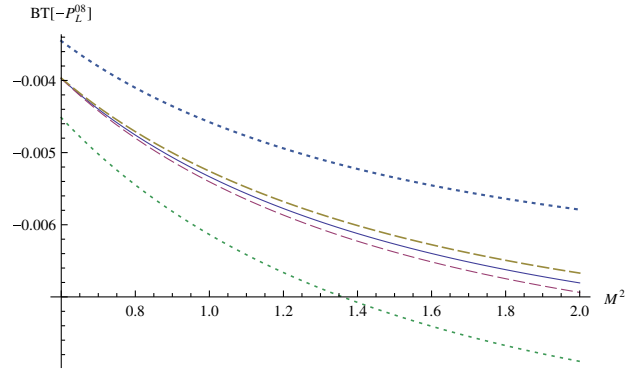

FIG. 11 (color online). Plots of $BT[-P_L^{08}]$ as a function of M^2 for normal (solid), α_s changed by 10% (dashed), and m_s changed by 10% (dotted).

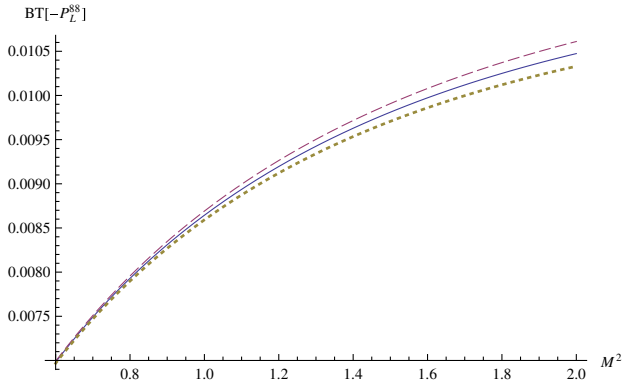

FIG. 9 (color online). Plots of $BT[-P_L^{88}]$ as a function of M^2 for $W^2 = 2.3$ GeV^2 (solid line), for $W^2 = 2.4$ GeV^2 (dashed line), and for $W^2 = 2.2$ GeV^2 (dotted line).

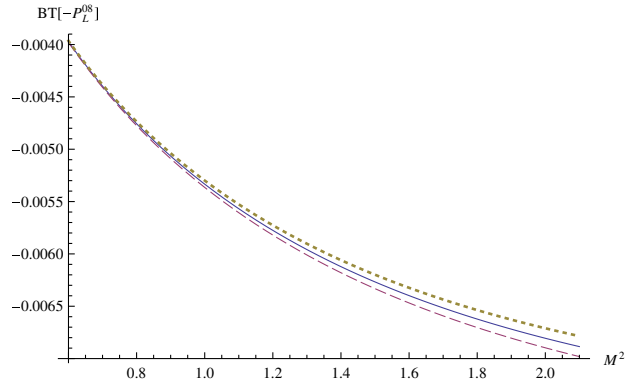

FIG. 12 (color online). Plots of $BT[-P_L^{08}]$ as a function of M^2 for $W^2 = 2.3$ GeV^2 (solid line), for $W^2 = 2.4$ GeV^2 (dashed line), and for $W^2 = 2.2$ GeV^2 (dotted line).

when the range of the Borel mass squared, M^2, over which fitting is carried out, is changed by ± 0.1 GeV^2 for both cases of $\mathrm{BT}[-P_L^{88}]$ and $\mathrm{BT}[-P_L^{08}]$. κ and κ_s appear in the matrix elements of the operators with the highest dimension used whose contributions to the sum rule happen to be less than 1%. Hence, the error due to the uncertainties in their values will be small. The errors arising due to the uncertainties in the numerical values of κ, κ_s as well as $\tilde{m}_\eta$ and $\tilde{m}_{\eta'}$ being small have been neglected. Our final result of this analysis is as follows:

$$
\begin{aligned}
m_q A_q \times 10^4\ (\mathrm{GeV}^3) &= 7.45^{+0.75}_{-0.69}(m_s)^{+0.14}_{-0.10}(\alpha_s)^{+0.05}_{-0.06}(\langle\bar{q}q\rangle)^{+0.08}_{+0.02}\left(\left\langle\frac{\alpha_s}{\pi}G^2\right\rangle\right)^{+0.65}_{-0.51}(W^2)^{+0.37}_{-0.39}(M^2),\\
m_q A'_q \times 10^4\ (\mathrm{GeV}^3) &= 5.53^{+0.57}_{-0.58}(m_s)^{+0.72}_{-0.63}(\alpha_s)^{+0.70}_{-0.60}(\langle\bar{q}q\rangle)^{+0.29}_{-0.63}\left(\left\langle\frac{\alpha_s}{\pi}G^2\right\rangle\right)^{+0.96}_{-0.74}(W^2)^{+1.12}_{-0.79}(M^2),\\
m_s A_s \times 10^2\ (\mathrm{GeV}^3) &= -2.841^{-0.286}_{+0.284}(m_s)^{-0.209}_{+0.225}(\alpha_s)^{-0.171}_{+0.151}(\langle\bar{q}q\rangle)^{-0.094}_{+0.101}\left(\left\langle\frac{\alpha_s}{\pi}G^2\right\rangle\right)^{-0.211}_{+0.245}(W^2)^{-0.305}_{+0.265}(M^2),\\
m_s A'_s \times 10^2\ (\mathrm{GeV}^3) &= 3.786^{+0.379}_{-0.378}(m_s)^{+0.143}_{-0.149}(\alpha_s)^{+0.104}_{-0.136}(\langle\bar{q}q\rangle)^{+0.036}_{-0.037}\left(\left\langle\frac{\alpha_s}{\pi}G^2\right\rangle\right)^{+0.427}_{-0.464}(W^2)^{+0.299}_{-0.402}(M^2),\\
A_G \times 10^2\ (\mathrm{GeV}^3) &= -2.197^{-0.201}_{+0.244}(m_s)^{-0.064}_{+0.043}(\alpha_s)^{-0.062}_{+0.075}(\langle\bar{q}q\rangle)^{-0.478}_{+0.280}\left(\left\langle\frac{\alpha_s}{\pi}G^2\right\rangle\right)^{-0.022}_{+0.258}(W^2)^{-0.127}_{-0.044}(M^2),\\
A'_G \times 10^2\ (\mathrm{GeV}^3) &= -3.704^{-0.251}_{+0.247}(m_s)^{-0.624}_{+0.581}(\alpha_s)^{-0.568}_{+0.299}(\langle\bar{q}q\rangle)^{-0.400}_{+0.271}\left(\left\langle\frac{\alpha_s}{\pi}G^2\right\rangle\right)^{-0.148}_{+0.539}(W^2)^{-0.400}_{+0.130}(M^2).
\end{aligned}
\tag{33}
$$

In Table I, we compare our results with those obtained by other authors. We give the total theoretical errors in our results of the matrix elements by adding the six individual theoretical errors, as given in Eq. (33), in quadrature. The maximum error, ~34%, is for $m_q A'_q$, while the minimum error, ~13%, is for $m_q A_q$.

While the authors of Refs. [4,6,8] use $1/N_C$ improved chiral perturbation theory and the FKS scheme [8] for η-η' mixing, GK [5] have used low-energy effective theory of QCD in the large-N_C limit with one mixing angle scheme for η-η' in the octet-singlet basis. Their results on matrix elements of pseudoscalar densities and anomaly are consistent with our results with error bars, except for A_G obtained by Feldmann [8], which is numerically smaller than our result. It may be pointed out that Feldmann has set up- and down-quark masses to zero for this derivation, which is equivalent to neglecting M_π^2 compared to M_K^2 in his derivation.

Pham [3] has used nonet symmetry for the matrix elements of the pseudoscalar densities in the η and η' states to calculate A_s and A'_s by extending the symmetry for the masses of pseudoscalar nonets that includes the effect of the $U(1)_A$ QCD anomaly. Results on A_G and A'_G obtained by Novikov *et al.* [19] are based on $SU(3)_{\mathrm{flavor}}$ symmetry and the QCD sum rule in the limit of $m_q = 0$ (q = u, d). These results for both pairs of the matrix elements agree with our results.

Cheng *et al.* [9] have introduced a new element, used neither by the other authors referenced in Table I nor in the present work, in the form of η-η'-G mixing, where G is the pseudoscalar glueball. The present work, based on the two-angle scheme for η-η' mixing in the octet-singlet basis and on the QCD sum rule approach, is also free of contamination of higher mass states due to the explicit use of continuum threshold. In addition, we have retained the three light quark masses as nonzero.

For many applications, it is convenient to introduce the quark flavor basis states:

$$
|\eta_q\rangle = \frac{1}{\sqrt{2}}|u\bar{u} + d\bar{d}\rangle, \qquad |\eta_s\rangle = |s\bar{s}\rangle. \tag{34}
$$

The physical states η and η' are related to the flavor states through a unitary matrix $U(\varphi)$ [[1,2,4]]:

$$
\begin{pmatrix} |\eta\rangle \\ |\eta'\rangle \end{pmatrix} = U(\varphi)\begin{pmatrix} |\eta_q\rangle \\ |\eta_s\rangle \end{pmatrix}, \tag{35}
$$

where

$$
U(\varphi) = \begin{pmatrix} \cos\varphi & -\sin\varphi \\ \sin\varphi & \cos\varphi \end{pmatrix}. \tag{36}
$$

TABLE I. Comparison of our results on pseudoscalar densities and anomaly matrix elements of η and η' mesons with those obtained by other authors (for Ref. [3], numerical evaluation was done by us).

Reference	$m_q A_q \times 10^4$ (GeV^3)	$m_q A'_q \times 10^4$ (GeV^3)	$m_s A_s \times 10^2$ (GeV^3)	$m_s A'_s \times 10^2$ (GeV^3)	$A_G \times 10^2$ (GeV^3)	$A'_G \times 10^2$ (GeV^3)
This work	$7.45^{+1.07}_{-0.95}$	$5.53^{+1.90}_{-1.63}$	$-2.84^{-0.55}_{+0.54}$	$3.79^{+0.67}_{-0.75}$	$-2.20^{-0.54}_{+0.46}$	$-3.70^{-1.06}_{+0.93}$
Gerard and Kou [5]	6.25	5.46	(-2.7 ± 0.4)	5.45 ± 0.8		
			(-2.9)	(3.45)		
Pham [3]			-2.52	3.63		
Cheng *et al.* [9]					-2.56	-5.4
					(-2.80)	(-5.7)
Novikov *et al.* [19]					-2.1	-3.5
AG [6]			-2.85	3.55		
BN [4]	3.54 ± 10.62	3.54 ± 7.08	-2.75	3.40	-2.2 ± 0.2	-5.7 ± 0.2
Feldmann [8]	7.07	5.66	-2.65	3.25	-1.2	-2.9

TABLE II. Values of our calculated matrix elements of quark pseudoscalar densities and anomaly operators (as given by central values in Table I) for quark flavor basis states.

Matrix elements	Values of matrix elements (GeV^3)
$\langle 0\|m_u\bar{u}i\gamma_5 u + m_d\bar{d}i\gamma_5 d\|\eta_q\rangle$	1.854×10^{-3}
$\langle 0\|m_u\bar{u}i\gamma_5 u + m_d\bar{d}i\gamma_5 d\|\eta_s\rangle$	-0.88×10^{-4}
$\langle 0\|m_s\bar{s}i\gamma_5 s\|\eta_s\rangle$	0.047317
$\langle 0\|m_s\bar{s}i\gamma_5 s\|\eta_q\rangle$	2.028×10^{-3}
$\langle 0\|\frac{\alpha_s}{4\pi}G^a_{\mu\nu}\tilde{G}^{a\mu\nu}\|\eta_q\rangle$	-0.040460
$\langle 0\|\frac{\alpha_s}{4\pi}G^a_{\mu\nu}\tilde{G}^{a\mu\nu}\|\eta_s\rangle$	-0.014698

In the singlet-octet basis, where the angles θ_0 and θ_8 are small and their difference is comparable to these angles themselves, it is pertinent to keep them distinct. On the other hand, in the quark flavor basis,

$$\left|\frac{\varphi_q - \varphi_s}{\varphi_q + \varphi_s}\right| \ll 1. \tag{37}$$

Hence, one generally deals with only one mixing angle $\varphi \cong \varphi_q \cong \varphi_s$ in this basis for the sake of convenience [8].

In Table II, we have displayed the matrix elements of quark pseudoscalar densities and anomaly operators for quark flavor basis states for $\varphi = 39.3°$ [1,4] using the central values of matrix elements given in Table I. We observe that OZI-preserving and OZI-violating matrix elements of pseudoscalar densities differ by an order of magnitude. This, again, indicates that the numerical values of A_s and A'_s will not be affected in a significant way when m_q is set to zero. Also, notice that the anomaly matrix element is larger for the state $|\eta_q\rangle$ than $|\eta_s\rangle$, since it is energetically favorable for gluons to pair produce lighter quarks.

In summary, current-current correlators using QCD sum rules give a reasonable estimate for the matrix elements of flavor-diagonal light quark pseudoscalar densities and axial anomaly operators between vacuum and η and η' meson states.

ACKNOWLEDGMENTS

Part of the work was done when the author was visiting the University of Oregon, Eugene. The author thanks the authorities of the University for their hospitality.

[1] Y.-Y. Charng, T. Kurimoto, and H.-n. Li, Phys. Rev. D **74**, 074024 (2006).
[2] J.-F. Hsu, Y.-Y. Charng, and H.-n. Li, Phys. Rev. D **78**, 014020 (2008).
[3] T. N. Pham, Phys. Rev. D **77**, 014024 (2008).
[4] M. Beneke and M. Neubert, Nucl. Phys. B **651**, 225 (2003).
[5] J.-M. Gerard and E. Kou, Phys. Rev. Lett. **97**, 261804 (2006).
[6] A. Ali and C. Greub, Phys. Rev. D **57**, 2996 (1998).
[7] A. G. Akeroyd, C. H. Chen, and C. Q. Geng, Phys. Rev. D **75**, 054003 (2007).
[8] T. Feldmann, Int. J. Mod. Phys. A **15**, 159 (2000).
[9] H.-Y. Cheng, H.-n. Li, and K.-F. Liu, Phys. Rev. D **79**, 014024 (2009).
[10] J. P. Singh and A. B. Patel, J. Phys. G **39**, 015006 (2012).
[11] J.-W. Chen, H.-M. Tsai, and K. C. Weng, Phys. Rev. D **73**, 054010 (2006).
[12] J. P. Singh and J. Pasupathy, Phys. Rev. D **79**, 116005 (2009).
[13] S. D. Bass, Phys. Scr. **T99**, 96 (2002); Acta Phys. Pol. B Proc. Suppl. **2**, 11 (2009).
[14] G. Veneziano, Nucl. Phys. **B159**, 213 (1979); E. Witten, Ann. Phys. (N.Y.) **128**, 363 (1980).
[15] P. Di Vecchia and G. Veneziano, Nucl. Phys. **B171**, 253 (1980).
[16] S. Weinberg, *The Quantum Theory of Fields* (Cambridge University Press, Cambridge, 1996).
[17] J. P. Singh and F. X. Lee, Phys. Rev. C **76**, 065210 (2007).
[18] B. L. Ioffe, V. S. Fadin, and L. N. Lipatov, *Quantum Chromodynamics: Perturbative and Nonperturbative Aspects* (Cambridge University Press, Cambridge, 2010).
[19] V. A. Novikov, M. A. Shifman, A. I. Vainshtein, and V. I. Zakharov, Nucl. Phys. **B165**, 55 (1980).